Am J Transl Res 2021;13(6):5866-5879
www.ajtr.org /ISSN:1943-8141/AJTR0124645

Original Article

ZNRD1-AS1 knockdown alleviates malignant phenotype of retinoblastoma through miR-128-3p/BMI1 axis

Guanghua Yang[1], Chen Zeng[1], Yang Liu[2], Dongliang Li[1], Juanjuan Cui[1]

[1]First Department of Oncology, Zhumadian Central Hospital, Zhumadian, Henan, China; [2]Department of Pediatric Oncology, Zhumadian Central Hospital, Zhumadian, Henan, China

Received October 21, 2020; Accepted April 20, 2021; Epub June 15, 2021; Published June 30, 2021

Abstract: Background: ZNRD1-AS1 plays an important role in liver cancer, endometrial cancer and other diseases. However, the relationship between ZNRD1-AS1 and retinoblastoma has not been studied in detail. This study aimed to determine the role of ZNRD1-AS1 in retinoblastoma. Methods: Differentially expressed genes in retinoblastoma downloaded from GEO database were identified by Limma package, and the expression and cell location of ZNRD1-AS1 were detected by real-time quantitative PCR (RT-qPCR). The relationships between miR-128-3p and two genes (ZNRD1-AS1 and BMI1) were analyzed by bioinformatics and dual-luciferase assay. After manipulating the expressions of ZNRD1-AS1, miR-128-3p and BMI1, cell viability, tube length, migration, invasion and the protein expressions (PCNA, E-Cadherin, N-Cadherin) of retinoblastoma cells were determined by cell counting kit-8 (CCK-8), tube formation, transwell and Western blot assays, respectively. Subcutaneous transplantation tumor assay, immunohistochemistry, and RT-qPCR were applied to verify the functions of the target gene *in vivo*. Results: ZNRD1-AS1 was up-regulated in the cytoplasm of retinoblastoma and regulated BMI1 via sponging miR-128-3p. ZNRD1-AS1 knockdown alleviated the malignant phenotype (viability, tube length, migration and invasion) of retinoblastoma cells, reduced tumor volume and weight, and inhibited BMI1 and CD34 expressions. Different from miR-128-3p mimic, miR-128-3p inhibitor promoted malignant phenotype of retinoblastoma cells, and partially reversed the inhibitory effect of siZNRD1-AS1. MiR-128-3p mimic down-regulated BMI1, PNCA, N-Cadherin expressions, and up-regulated p16 and E-Cadherin expressions. The regulatory effect of miR-128-3p was partially reversed by BMI1. Conclusion: ZNRD1-AS1, acting as a "sponge" of miR-128-3p, up-regulates BMI1, thereby promoting the progression of retinoblastoma.

Keywords: Retinoblastoma, ZNRD1-AS1, miR-128-3p, BMI1, biological characteristics

Introduction

Retinoblastoma is a common intraocular malignant tumor among children, with approximately an estimated 8,000 new cases of child retinoblastoma diagnosed each year [1]. Traditional therapies for retinoblastoma, such as eyeball enucleation, external radiotherapy or chemotherapy, and laser therapy are often complicated with infection, disfigurement, blindness and some other adverse reactions; moreover, most of the patients tended to develop a poor prognosis [2, 3]. Continuous improvement of clinical treatment provides more options of diagnosis and retinoblastoma treatment [4], with the goal shifting from protecting the lives of diseased children to improving their life quality [5]. Therefore, it is particularly important to study the molecular biological mechanism underlying the occurrence and development of retinoblastoma and to identify tumor markers for an early diagnosis of retinoblastoma.

Some long non-coding RNAs (lncRNAs) are abnormally expressed in limited areas of retinal tissues, and have important regulatory effects on the development and pathology of the retina [6, 7]. In particular, Liu et al. proved that RNCR3 knockdown significantly inhibited the proliferation of retinal glial cells [8]. MALAT1 can regulate endothelial cell functions in diabetic retinopathy and promote cell proliferation through the p38/MAPK signaling pathway. Down-regulation of MALAT1 expression significantly reduces the inflammatory response of the retina [9]. Retinoblastoma is an embryonic

malignant tumor that originates from primitive stem cells in the nuclear layer of the retina [1]. Studying the role of lncRNAs in retinoblastoma has also been conducted previously [10]. For example, Su et al. found that lncRNA-BANCR is overexpressed in retinoblastoma tissues and cell lines, and is related to tumor size, choroidal infiltration and optic nerve invasion [11]. Down-regulating HOTAIR can inhibit the proliferation of retinoblastoma cells, and cause the G0/G1 phase arrest possibly through promoting the proliferation and invasion of tumor cells by activating the Notch signaling pathway [12]. Based on the above studies, we speculated that lncRNAs play a certain role in the development of retinoblastoma.

By applying bioinformatics and performing molecular experiments, we found that zinc ribbon domain-containing 1 antisense RNA 1 (ZNRD1-AS1) was differentially expressed in retinoblastoma. Recent studies indicated that ZNRD1-AS1 has an important regulatory effect on liver cancer, endometrial cancer and some other diseases [13, 14]. As there is a lack of data on the association between ZNRD1-AS1 and retinoblastoma, the present study was designed to determine the effect of ZNRD1-AS1 on retinoblastoma.

Materials and methods

Ethics statement

Approval for conducting this study was obtained from the Ethics Committee of Zhumadian Central Hospital (RE202003028). All the tissues were acquired from patients who were clinically diagnosed with retinoblastoma or from normal subjects. Written informed consents were obtained from all the participants.

Animal protocols were carried out according to the guidelines formulated by the China Council on Animal Care and Use, and were approved by the committee of experimental animals of our hospital (DB202004024). The mice were raised in a pathogen-free animal facility, with standard pellet diet and water provided.

Cells and culture

Normal retinal pigment epithelial cell line ARPE-19 (CRL-2302), retinoblastoma cells Weri-Rb1 (HTB-169) and Y79 (HTB-18), DMEM medium (30-2006), and fetal bovine serum (FBS) (30-2020) were purchased from American Type Culture Collection (USA). SO-RB50 cells were purchased from ChemicalBook Company (China), and HXO-RB44 cells were purchased from Shanghai Institute of Biochemistry and Cell Biology (CAS). The cells were cultivated in DMEM medium supplemented with 10% FBS in a 5% CO_2 incubator (SCO6WE-2, SHELLAB, USA) at 37°C.

Transfection

The siRNA targeting ZNRD1-AS1 (siZNRD1-AS1, target sequence: AGCACAAAATTGGTAACCAATGC), shRNA targeting ZNRD1-AS1 (shZNRD1-AS1, target sequence: GCACCCAATCCTGGGATATTT), and BMI1 overexpression plasmid were commercially ordered from GenePharma Company (China). miR-128-3p mimic or inhibitor (M/I, miR10000424-1-5/miR20000424-1-5) and mimic or inhibitor control (MC/IC, miR1N0000002-1-5/miR2N0000002-1-5) were purchased from RIBOBIO Company (China). RNA and plasmids were transfected into retinoblastoma cells with Lipofectamine 3000 (L3000015, Invitrogen, USA), and siRNAs were transfected by Lipofectamine RNAiMAX Transfection Reagent (13778030, Invitrogen, USA).

Real-time quantitative PCR (RT-qPCR)

Sample RNAs were collected using TRIzol reagent (15596018, Invitrogen, USA). Cytoplasm and nucleus RNAs were extracted by Cytoplasmic & Nuclear RNA Purification Kit (NGB-21000, NorgenBiotek, Canada). NanoDrop One machine (Thermo, USA) was employed to measure RNA purity and concentration. The synthesis of cDNA was performed according to the instructions of lncRNA cDNA first strand synthesis kit (KR202, TIANGEN, China), miRNA cDNA Kit (KR211, TIANGEN, China) or FastKing one-step RT-PCR kit (KR123 TIANGEN, China). Subsequently, qPCR was operated in ABI 7500 real-time PCR system (Applied Biosystems, USA) with FastFire qPCR PreMix (FP207, TIANGEN, China) or GeneCopoeia miRNA qPCR Kit (QM001, China). U6 or GAPDH served as internal reference. Gene expressions were calculated by $2^{-\Delta\Delta Ct}$ method [15]. All the primer sequences were listed as follows (5'-3'): ZNRD1-AS1: TTTTGTCACTTCCTATCACCCAC, GCTGAGTTTGATTATCCCTGAGTG; miR-128-3p: GGTCACAGTGAACCGGTC, GTGCAGGGTCCGAGGT; BMI1:

CCACCTGATGTGTGTGCTTTG, TTCAGTAGTGGTCTGGTCTTGT; GAPDH: TGTTCGTCATGGGTGTGAAC, ATGGCATGGACTGTGGTCAT; U6: CTCGCTTCGGCAGCACA, AACGCTTCACGAATTTGCGT.

Cell counting kit-8 (CCK-8) assay

Cell viability of retinoblastoma was determined by CCK-8 (96992, Sigma-Aldrich, USA). Weri-Rb1 or Y79 cells (approximately 1×10^3/well) were incubated for 24, 48, or 72 hours (h). At each time point, CCK-8 solution (10 μL) was added into cells for further 2-h cultured at 37°C. After that, cell viabilities (optical density at 450 nm) were determined by a microplate reader (EnVision, PerkinElmer, USA).

Tube formation

Briefly, retinoblastoma cells were co-cultured with HUVECs (PCS-100-013, ATCC, USA) for 24 h, and then HUVECs were collected for tube formation assays. The HUVECs (1×10^4 cells/well) were seeded to a 96-well culture plate pre-coated with Matrigel (354230, BD Biosciences, USA). After routine culture of the cells for 4-6 h, tube lengths were calculated with a Nikon ECLIPSE Ts2 microscope (Japan) (magnification ×100).

Transwell assay

The migration and invasion of retinoblastoma cells were assessed with Transwell assays. Cell suspensions (1×10^3/well) were added into the upper chamber of Transwell (3422, Corning, USA) covered with Matrigel (354230, BD, USA, for invasion) or without (for migration), while the medium containing 10% FBS was added to the lower chamber. Then, after incubating the cells for 48 h, cells migrated or invaded through the membrane were stained with 0.1% crystal violet (V5265, Sigma-Aldrich, USA), imaged and counted with a Nikon ECLIPSE Ts2 microscope (Japan, magnification ×100).

Bioinformatics assay and dual luciferase assay

Retinoblastoma gene expression data were downloaded from NCBI Gene Expression Omnibus (GEO) dataset (GSE125903), and the Limma software package was used for differential gene analysis. Differentially expressed genes were then visualized by volcano map and heat map. The binding sites between ZNRD1-AS1 and miR-128-3p, and the target relationship between miR-128-3p and BMI1 were predicted on starBase v2.0 (http://starbase.sysu.edu.cn/index.php).

To analyze the relationship between ZNRD1-AS1 and miR-128-3p as well as between miR-128-3p and BMI1, the miR-128-3p M or MC was synthesized, and co-transfected with wild-type and mutant ZNRD1-AS1 or BMI1 recombinant plasmid (pmirGLO, E1330, Promega, USA) into Weri-Rb1 and Y79 cells. Finally, relative luciferase activities were examined using a dual-luciferase detection kit (E1910, Promega, USA).

Western blot

Total proteins of Weri-Rb1 or Y79 cells were extracted using RIPA lysis buffer (P0013B, Beyotime Company, China) with protease inhibitors (P1005, Beyotime Company, China) and PMSF (ST505, Beyotime Company, China), followed by quantification of protein content with bicinchoninic acid (BCA) kit (P0011, Beyotime, China). Equivalent amounts of total proteins were separated by sodium dodecyl sulfate polyacrylamide gel electrophoresis (SDS-PAGE). Next, the proteins were transferred to the polyvinylidene fluoride (PVDF) membranes (160-0184, BIO-RAD, USA), which were then blocked for 1 h. Afterwards, the membranes were incubated with primary antibodies against BMI1 (ab14389, 37 kDa, 1 μg/mL, Abcam, UK), p16 (ab201980, 17 kDa, 1/1000, Abcam, UK), PNCA (ab92552, 29 kDa, 1/1000, Abcam, UK), E-Cadherin (ab40772, 97 kDa, 1/10000, Abcam, UK), N-Cadherin (ab18203, 130 kDa, 1 μg/mL, Abcam, UK) and GADPH (ab181602, 1/10000, 36 kDa, Abcam, UK), and then incubated with HRP-labeled secondary antibody rabbit IgG (ab205718). Finally, the protein bands were developed by ECL chemiluminescent solution (PE0010, Solarbio, China) and analyzed by analysis software (Quantity One 1-D, Bio-Rad Laboratories, USA).

Tumorigenesis assay

BALB/c male nude mice (4-6 weeks old, 211) were purchased from Charles River Company (China). All the mice were randomly divided into shNC (n = 6) and shZNRD1-AS1 groups (n = 6). Part of the mice were injected subcutaneously with 2×10^5/mL Weri-Rb1 cells transfected with shNC, while the rest of the mice were subcuta-

neously injected with 2×10^5/mL Weri-Rb1 cells transfected with shZNRD1-AS1, and then routinely raised. Tumor formation was constantly observed. When the tumor volume in the shNC group reached approximately 1000 mm^3, the two groups of mice were euthanized with intraperitoneal injection of sodium pentobarbital (150 mg/kg, P3761, Sigma-Aldrich, USA), and their tumor volume and weight were recorded. Thereafter, tumor images were captured and recorded, and the tumor tissues were collected for later use.

Immunohistochemistry (IHC)

IHC was performed to determine the expressions of BMI1 and blood vessel density marker CD34 in tumor tissues. Tumor samples were prepared using Richard-Allan Scientific Signature Series Pen-Fix (6105, Thermo Scientific, USA), and then the antigen was recovered by IHC Antigen Retrieval Solution (00-4955-58, eBioscience, USA), followed by background blocking with IHC/ICC blocking buffer (00-4953-54, eBioscience, USA). Next, the target signals were detected and visualized by Western blot. Anti-BMI1 (ab269678, 1 μg/mL) and anti-CD34 (ab81289, 1/2500) from Abcam (UK) were used to detect target genes.

Data analysis

The data were presented by mean ± standard deviation, and GraphPad Prism 8.0 (Graphpad software, USA) was used for statistical analysis. The independent sample *t* test was used for comparison between the two groups while paired sample *t* test was used for comparison between cancerous tissues and adjacent tissues. Comparison between multiple groups was conducted by one-way ANOVA. $P < 0.05$ was defined as statistically significant.

Results

ZNRD1-AS1 was up-regulated in retinoblastoma

Retinoblastoma gene expression data (GSE125903) was downloaded from the GEO database, and analyzed by the Limma package for differentially expressed genes. As shown in **Figure 1A**, **1B**, among the differentially expressed genes screened, there were 427 up-regulated genes and 503 down-regulated genes. Subsequently, we determined the expression of ZNRD1-AS1 in retinoblastoma tissues (n = 40) and found that ZNRD1-AS1 expression was up-regulated in cancer tissues ($P < 0.001$, **Figure 1C**). We also found that the expressions of ZNRD1-AS1 in retinoblastoma Weri-Rb1, Y79, SO-RB50, and HXO-RB44 cells were significantly higher than that of normal retinal pigment epithelial cell line (ARPE-19) ($P < 0.001$, **Figure 1D**). Moreover, the expression of ZNRD1-AS1 in Weri-Rb1 and Y79 cells was higher than that of other cancer cell lines. Thus, the two cells were therefore selected as the experiment cells.

SiZNRD1-AS1 alleviated the malignant phenotype of retinoblastoma cells

To investigate whether ZNRD1-AS1 could affect the biological behaviors of retinoblastoma cells, we transfected siZNRD1-AS1 into Weri-Rb1 and Y79 cells and found that siZNRD1-AS1 significantly down-regulated the expression of ZNRD1-AS1 ($P < 0.001$, **Figure 2A**). Moreover, siZNRD1-AS1 greatly inhibited cell viability ($P < 0.01$, **Figure 1B**). siZNRD1-AS1 notably reduced tube length, as shown in **Figure 2C**, **2D** ($P < 0.001$). Transwell results demonstrated that the migration and invasion of siZNRD1-AS1 group were observably lower than that of siNC group ($P < 0.001$, **Figure 2E-H**).

SiZNRD1-AS1 interfered with the malignant phenotype of retinoblastoma cells through miR-128-3p

LncRNAs play different roles in different locations of cell. Generally, cytoplasmic lncRNAs exert their effects through regulating miRNAs. To study the cellular localization of ZNRD1-AS1, we determined its expression in the cytoplasm and nucleus and found that ZNRD1-AS1 was mainly expressed in the cytoplasm (**Figure 3A**). MiR-128-3p was predicted to be the targeted miRNA of ZNRD1-AS1 ($P < 0.001$, **Figure 3B**, **3C**). SiZNRD1-AS1 remarkably up-regulated miR-128-3p expression in Weri-Rb1 and Y79 cells, suggesting that ZNRD1-AS1 may act as a sponge to miR-128-3p ($P < 0.001$, **Figure 3D**).

To verify our speculation, we conducted a rescue experiment. MiR-128-3p mimic up-regulated the expression of miR-128-3p, but miR-128-3p inhibitor down-regulated miR-128-3p, partially counteracting the promoting effect of siZNRD1-AS1 ($P < 0.05$, **Figure 4A**). Additionally, different from miR-128-3p mimic, miR-128-3p

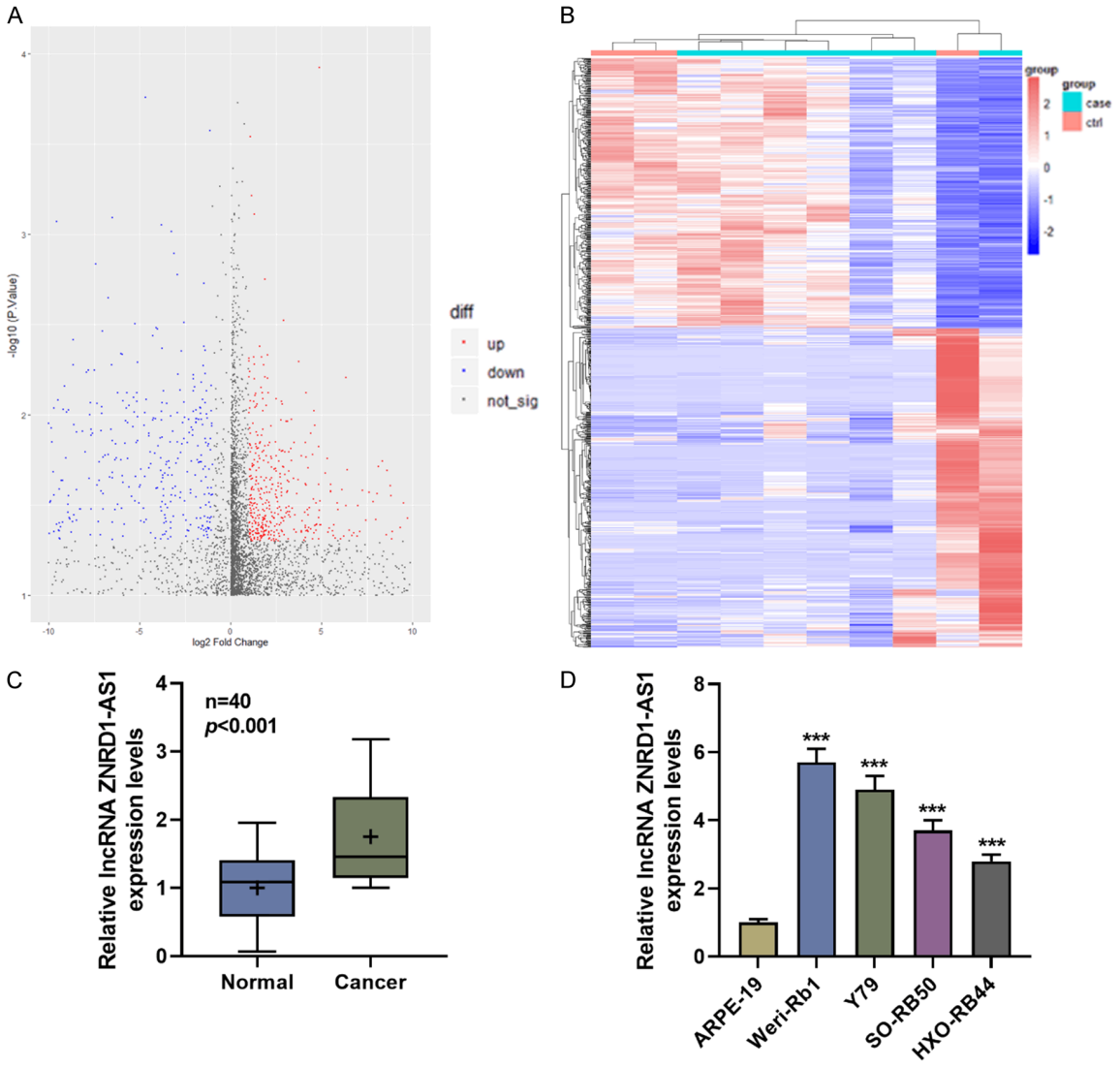

Figure 1. ZNRD1-AS1 was up-regulated in retinoblastoma. A, B. Scatter plots and heat maps of differentially expressed genes in retinoblastoma (427 up-regulated genes and 503 down-regulated genes). C, D. RT-qPCR was performed to detect the expression of ZNRD1-AS1 in retinoblastoma tissues and cells. RT-qPCR: Real-time quantitative PCR. Experiments were repeated in triplicates. $^{***}P < 0.001$ vs. ARPE-19.

inhibitor increased cell viability, tube length, migration and invasion rates, and partially overturned the inhibitory effect of siZNRD1-AS1 ($P < 0.05$, **Figure 4C-H**).

MiR-128-3p regulated the biological behaviors of retinoblastoma cells through BMI1

Figure 5A, **5B** show that miR-128-3p could directly target BMI1 ($P < 0.01$). Moreover, the up-regulated expression of BMI1 by its overexpression plasmid was inhibited by miR-128-3p mimic in Weri-Rb1 and Y79 cells ($P < 0.05$, **Figure 5C**). However, overexpressed BMI1 had no significant effect on miR-128-3p, while miR-128-3p mimic up-regulated miR-128-3p, suggesting that BMI1 was a downstream gene of miR-128-3p ($P < 0.001$, **Figure 5D**). Subsequently, functional tests demonstrated that BMI1 partially reversed the inhibitory effects of miR-128-3p mimic on cell viability, tube length, migration and invasion of Weri-Rb1 and Y79 cells ($P < 0.05$, **Figures 5E**, **6A-F**).

In addition, the expressions of proteins related to BMI1/p16 pathway, proliferation, migration

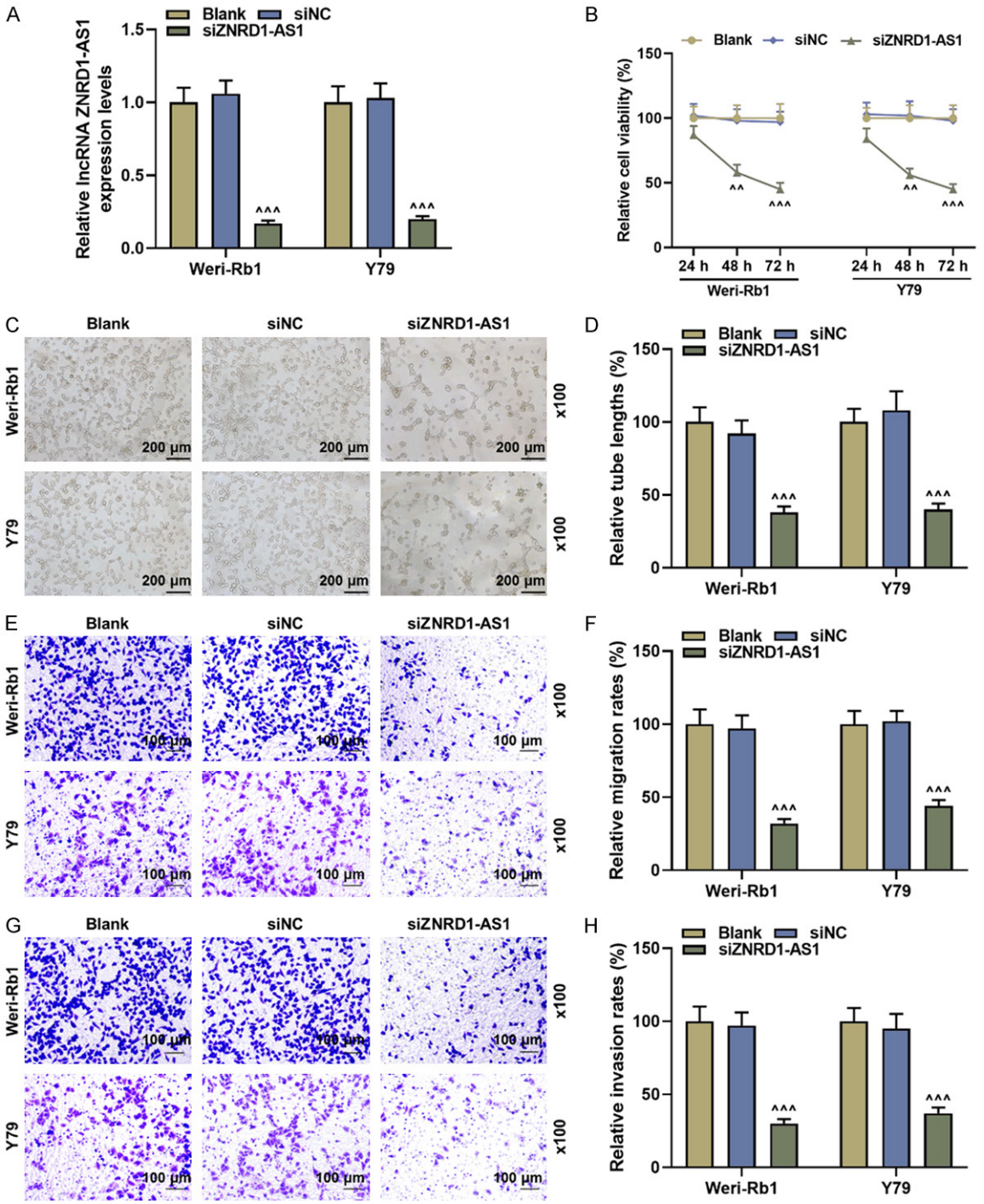

Figure 2. SiZNRD1-AS1 alleviated the malignant phenotype of retinoblastoma cells. A. SiRNA targeting ZNRD1-AS1 was transfected into Weri-Rb1 or Y79 cells, and RT-qPCR was performed to detect the transfection rate. B. The effect of ZNRD1-AS1 silence on cell viability was determined by CCK-8. C, D. The tube length of blank, siNC, and siZNRD1-AS1 groups was determined by the tube formation assay. E-H. Transwell assay was used to evaluate the effects of ZNRD1-AS1 silence on cell migration and invasion. ^^$P < 0.01$, ^^^$P < 0.001$ vs. siNC.

and invasion in each group were determined, and we observed that miR-128-3p mimic down-regulated the expressions of BMI1, PNCA, and N-Cadherin, and up-regulated expressions of p16 and E-Cadherin ($P < 0.05$, **Figure 7A-D**). The regulatory effect of BMI1 on the above-

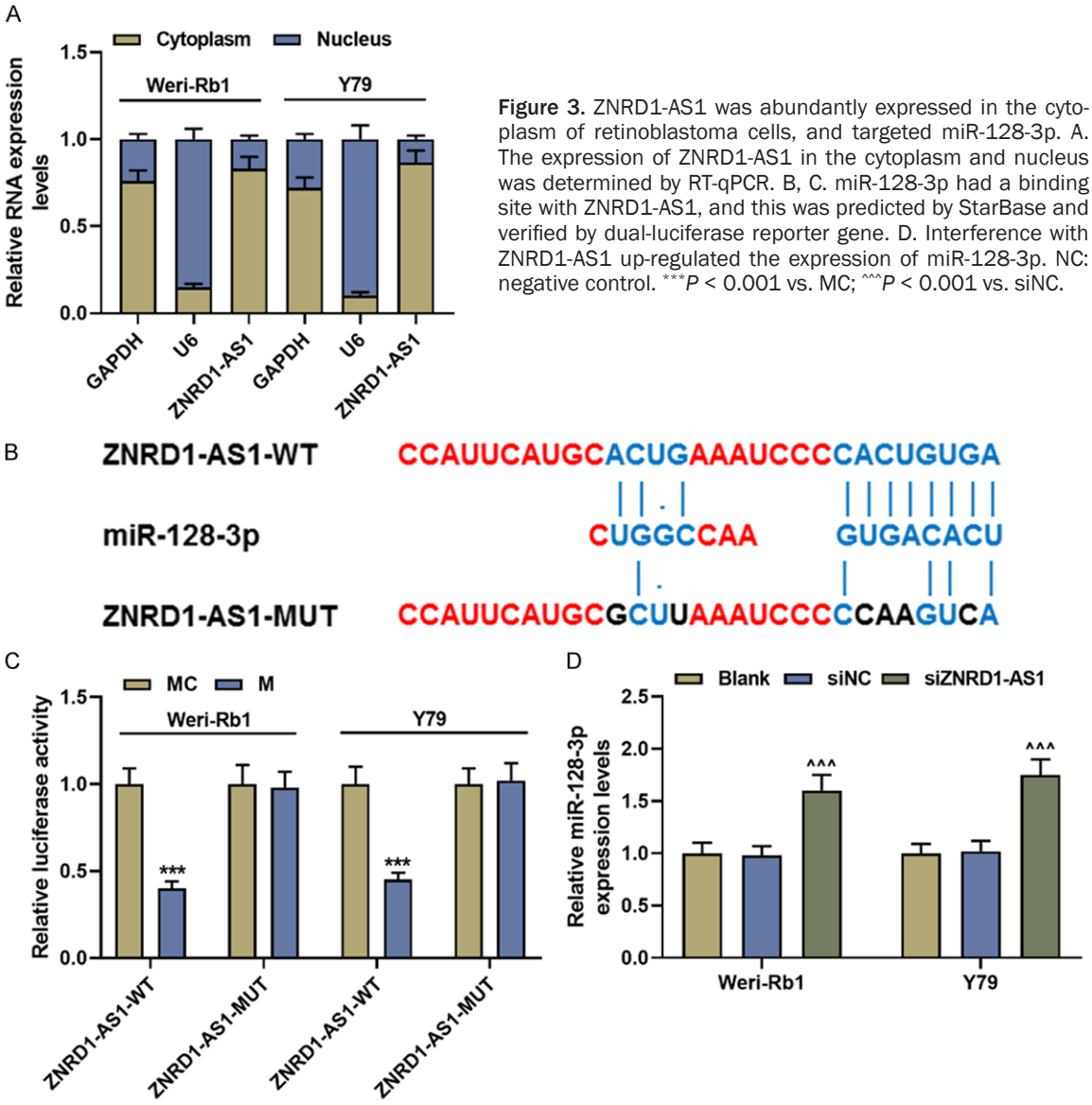

Figure 3. ZNRD1-AS1 was abundantly expressed in the cytoplasm of retinoblastoma cells, and targeted miR-128-3p. A. The expression of ZNRD1-AS1 in the cytoplasm and nucleus was determined by RT-qPCR. B, C. miR-128-3p had a binding site with ZNRD1-AS1, and this was predicted by StarBase and verified by dual-luciferase reporter gene. D. Interference with ZNRD1-AS1 up-regulated the expression of miR-128-3p. NC: negative control. $^{***}P < 0.001$ vs. MC; $^{\wedge\wedge\wedge}P < 0.001$ vs. siNC.

mentioned genes was the opposite, partially reversing the effect of miR-128-3p mimic ($P < 0.05$, **Figure 7A-D**).

Silencing ZNRD1-AS1 inhibited tumor growth via miR-128-3p/BMI1

In order to verify the *in vitro* results, a subcutaneous xenograft assay was constructed. As shown in **Figure 8A-C**, shZNRD1-AS1 sharply reduced tumor volume and weight ($P < 0.001$). Next, we found that shZNRD1-AS1 significantly down-regulated BMI1 (**Figure 8D**). Immunohistochemistry results indicated that the level of CD34 in the shZNRD1-AS1 group was noticeably lower than that in the shNC group (**Figure 8E**). In addition, in tumor tissues, we verified that shZNRD1-AS1 inhibited miR-128-3p but promoted ZNRD1-AS1 expression ($P < 0.001$, **Figure 8F-G**).

Discussion

Molecular targeted therapy provides new possibilities for the treatment of retinoblastoma [16]. However, the mechanism of occurrence and development of retinoblastoma is still unclear, which requires a better understanding of the pathogenic mechanism of retinoblastoma to help find new diagnostic markers for

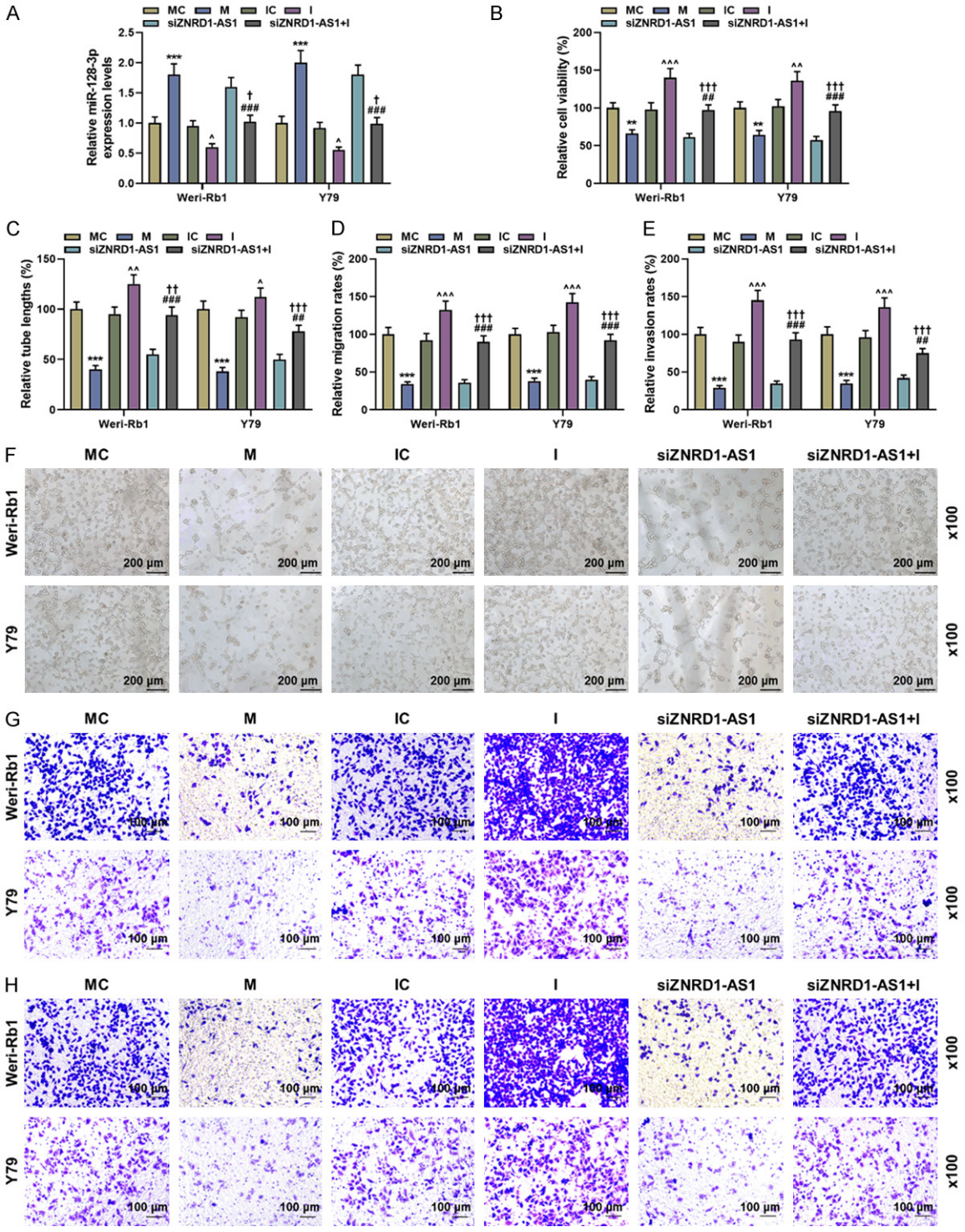

Figure 4. The inhibitory effect of siZNRD1-AS1 on the malignant phenotype of retinoblastoma cells was reversed by miR-128-3p inhibitor. A. The effects of siZNRD1-AS1 and miR-128-3p on miR-128-3p were examined by RT-qPCR. B. CCK-8 detected the cell viability of mimic control (MC), mimics (M), inhibitor control (IC), inhibitors (I), siZNRD1-AS1, siZNRD1-AS1+I groups. C-E. Statistical histograms of tube length, migration and invasion in each group. F. Diagram of tube formation in each group. G, H. Maps of migration and invasion cells formed by each group of Transwell assay. $^{**}P < 0.01$, $^{***}P < 0.001$ vs. MC; $^{\wedge}P < 0.05$, $^{\wedge\wedge}P < 0.01$, $^{\wedge\wedge\wedge}P < 0.001$ vs. IC; $^{\#\#}P < 0.01$, $^{\#\#\#}P < 0.001$ vs. siZNRD1-AS1; $^{\dagger}P < 0.05$, $^{\dagger\dagger}P < 0.01$, $^{\dagger\dagger\dagger}P < 0.001$ vs. I.

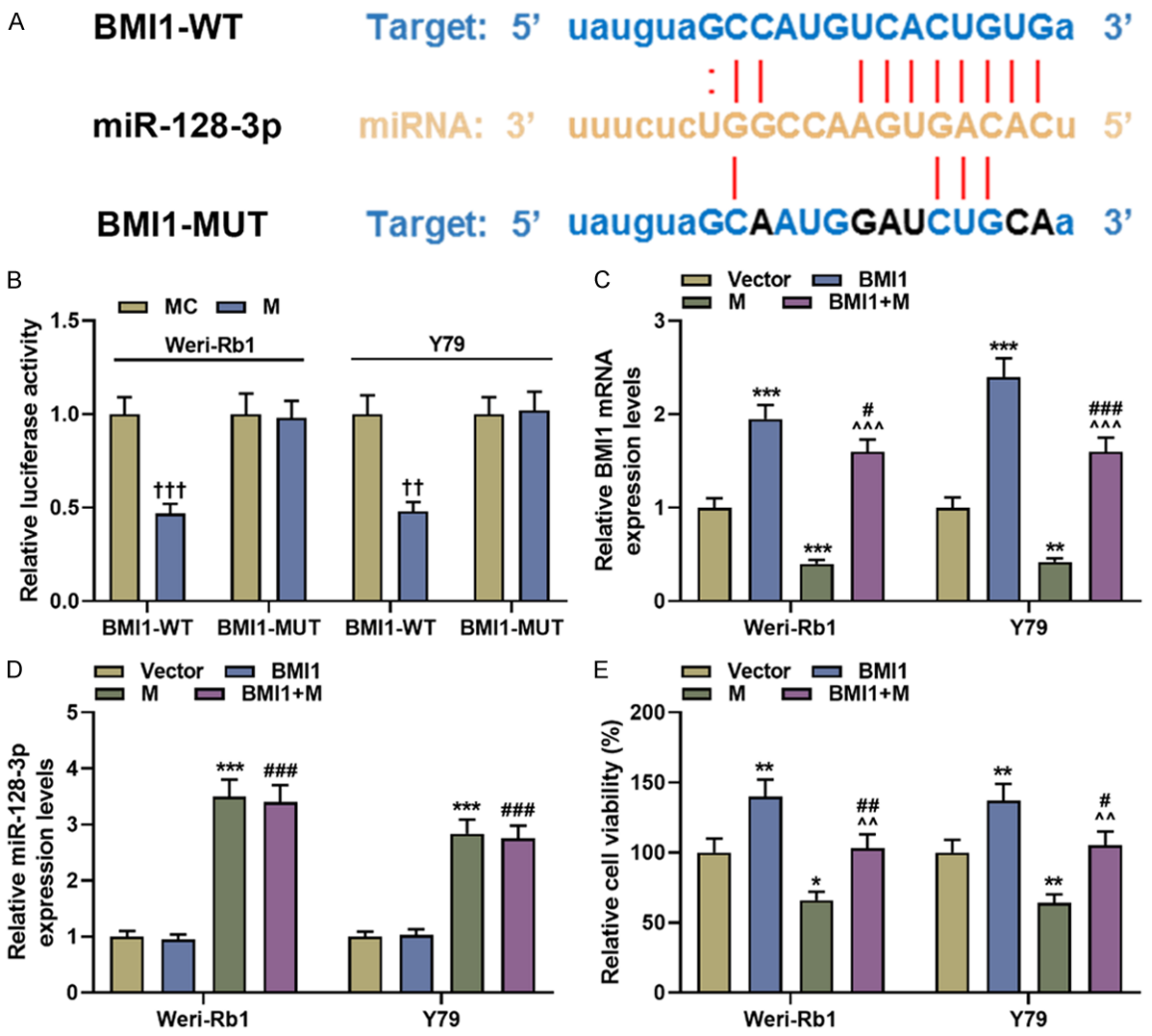

Figure 5. BMI1 was a downstream target gene of miR-128-3p. A, B. StarBase and dual-luciferase reporter gene were used to analyze the binding relationship between BMI1 and miR-128-3p. C, D. The expressions of BMI1 and miR-128-3p in vector, BMI1, mimic (M), and BMI1+M groups were evaluated by RT-qPCR. E. Cell counting Kit-8 (CCK-8) was used to detect cell viability. $^{††}P < 0.01$, $^{†††}P < 0.001$ vs. MC; $^{**}P < 0.01$, $^{***}P < 0.001$ vs. vector; $^{\wedge\wedge}P < 0.01$, $^{\wedge\wedge\wedge}P < 0.001$ vs. M; $^{\#}P < 0.05$, $^{\#\#}P < 0.01$, $^{\#\#\#}P < 0.001$ vs. BMI1.

retinoblastoma and possible new targets for tumor molecular therapy. In our study, ZNRD1-AS1 acted as a sponge of miR-128-3p by up-regulating BMI1 to promote the progression of retinoblastoma.

ZNRD1-AS1 is the upstream lncRNA of ZNRD1 [17]. As it is a relatively novel lncRNA, studies on ZNRD1-AS1 at present are limited. Recently, some studies have examined the functions of ZNRD1-AS1 in nasopharyngeal carcinoma, breast cancer, glioma, etc. [15, 18, 19]. Wang et al. confirmed that ZNRD1-AS1 expression is up-regulated in nasopharyngeal carcinoma (NPC) tissues and cells, and silencing ZNRD1-AS1 can inhibit the invasion of NPC cells [15]. Our results also showed similar expression of ZNRD1-AS1 in retinoblastoma, suggesting that ZNRD1-AS1 may play a carcinogenic role in retinoblastoma. The latest study in bladder cancer found that ZNRD1-AS1 silencing inhibited the proliferation, metastasis and epithelial-mesenchymal transition (EMT) of bladder cancer cells [20]. The above findings indicated that ZNRD1-AS1 could promote tumor progression in a variety of cancers.

The regulatory mechanism of lncRNA varies in many aspects [21]. For example, lncRNAs can act as competing endogenous RNAs (ceRNAs)

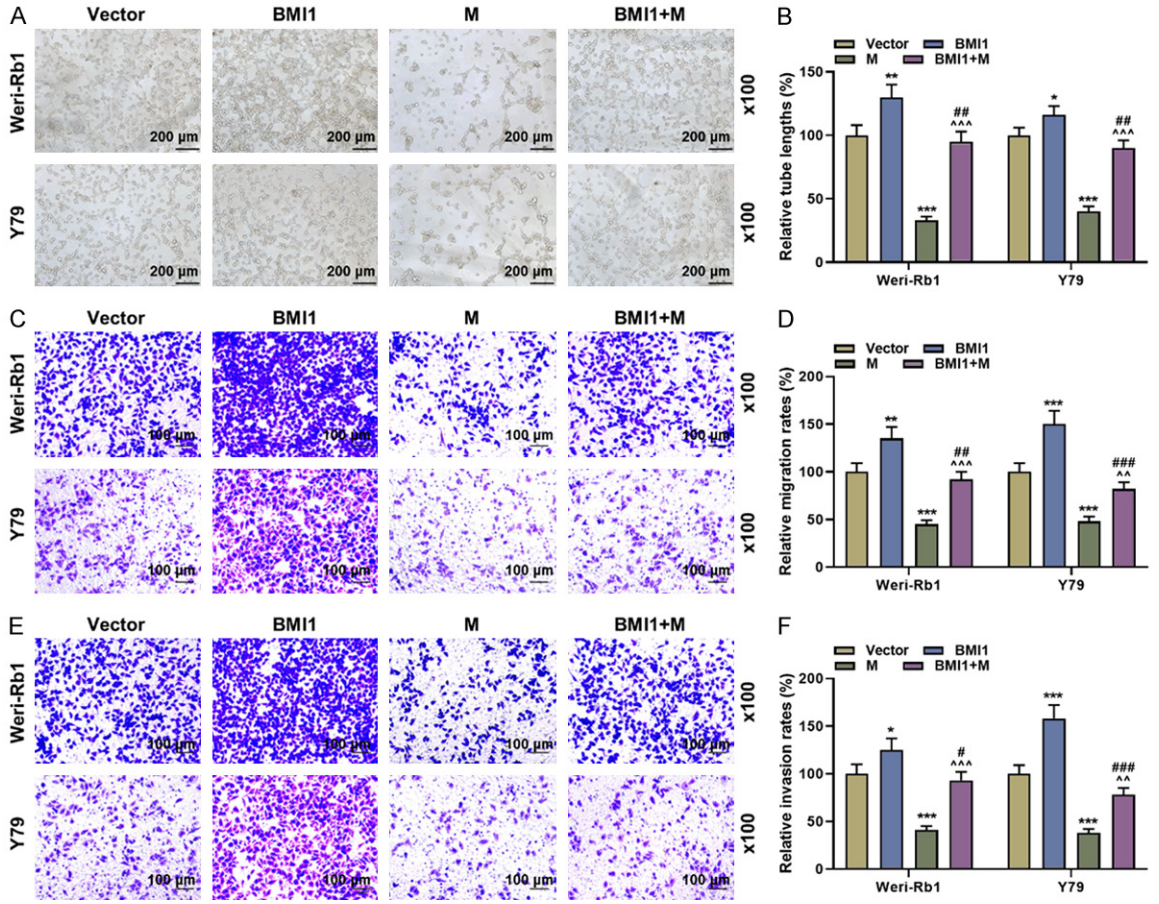

Figure 6. The promoting effect of miR-128-3p mimics on the biological phenotype was reversed by BMI1. A and B. The tube lengths of the vector, BMI1, M, and BMI1+M groups were evaluated by the tube formation assay. C-F. The migration and invasion of each group of cells were measured by Transwell assay. $^{*}P < 0.05$, $^{**}P < 0.01$, $^{***}P < 0.001$ vs. vector; $^{\wedge\wedge}P < 0.01$, $^{\wedge\wedge\wedge}P < 0.001$ vs. M; $^{\#}P < 0.05$, $^{\#\#}P < 0.01$, $^{\#\#\#}P < 0.001$ vs. BMI1.

by competitively binding to miRNA, thereby promoting the translation of corresponding mRNAs. Direct binding of lncRNAs to DNA methyltransferase (DNMT) could inhibit the methylation of gene promoters. lncRNAs can also act as precursors of some miRNAs to regulate gene expressions [22, 23]. Wang et al. analysis showed that as a ceRNA, ZNRD1-AS1 promotes the invasion and metastasis of NPC cells through the miR-335-ROCK1 axis [15]. Some scholars also pointed out that ZNRD1-AS1 acts as a ceRNA to up-regulate the expression of ELF1 by binding with miR-499a-5p, thereby promoting the angiogenesis mimicry of glioma cells [18]. Our research found that ZNRD1-AS1 also acts as a ceRNA in retinoblastoma, and it can competitively bind miR-128-3p to promote cell tube formation, migration and invasion.

A number of studies reported that miR-128-3p acts as a tumor suppressor gene to regulate the occurrence and development of tumors [24, 25]. Moreover, miR-128 has been found to be down-regulated in lung cancer, pancreatic cancer and other malignant tumors [26, 27]. In this study, we found that up-regulation of miR-128-3p noticeably attenuated the malignant phenotype of retinoblastoma cells, and down-regulation of miR-128-3p promoted the malignant progression of cells. MiRNAs, a group of small RNA molecule in cells, inhibit translation process by incomplete complementary binding to the mRNA sequence of its target gene, thereby down-regulating the expression of the target gene and achieving gene silencing [28]. Liu et al. showed that [24] miR-128-3p targets the 3'UTR region of BMI1, and miR-128-3p overexpression up-regulates E-cadherin and inhibits

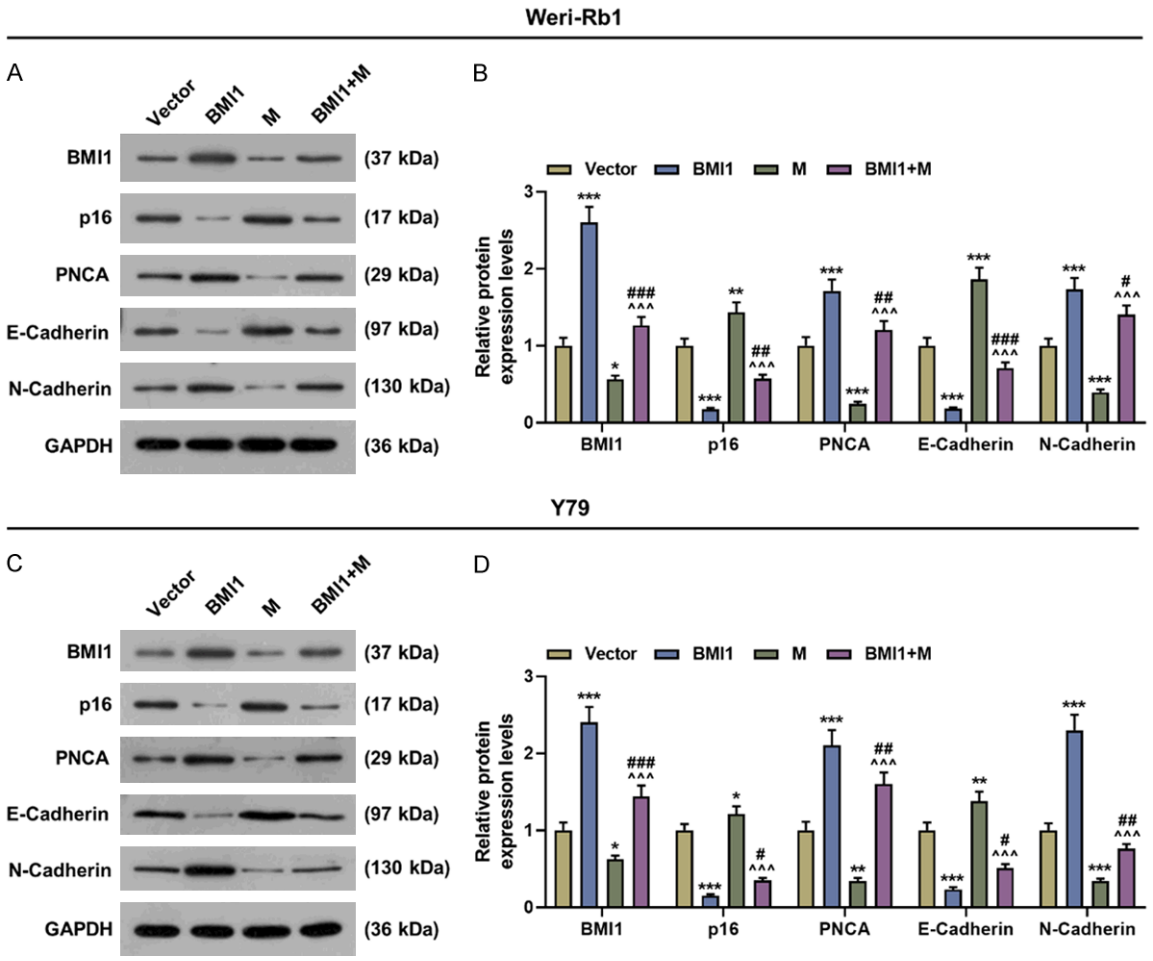

Figure 7. The related protein expressions of BMI1/p16 pathway and proliferation, migration and invasion in vector, BMI1, M, and BMI1+M groups were detected by Western blot. GAPDH was a control. $^{*}P < 0.05$, $^{**}P < 0.01$, $^{***}P < 0.001$ vs. vector; $^{\wedge\wedge\wedge}P < 0.001$ vs. M; $^{\#}P < 0.05$, $^{\#\#}P < 0.01$, $^{\#\#\#}P < 0.001$ vs. BMI1.

oxaliplatin-induced EMT by suppressing Bmi1 expression in resistant cells. We also confirmed that BMI1 is a downstream target gene of miR-128-3p.

Evidence increasingly supported that the regulation of BMI1 is related to the EMT and invasive development of cancers [30-32]. Moreover, down-regulation of BMI1 also inhibits growth of retinoblastoma Y79 cells [37]. BMI1 regulates cell cycle progression and prevents cell senescence through inhibiting p16/Rb and p19/p53 pathways [38]. Our research also showed that overexpression of BMI1 promoted the malignant biological behaviors of retinoblastoma, inhibited p16, and up-regulated the expressions of PNCA and EMT-related proteins. EMT is an important process of the development of tumors, and detecting the expression of EMT-related proteins helps understand the regulatory mechanism of tumors [39]. Interestingly, we found that overexpression of BMI1 partially counteracted the effect of miR-128-3p mimic on retinoblastoma cells. In addition, *in vivo* experiments also proved that ZNRD1-AS1 can inhibit tumor growth and angiogenesis via miR-128-3p/BMI1 axis. Our next research will be based on the current findings and conduct animal experiments.

Disclosure of conflict of interest

None.

Address correspondence to: Guanghua Yang, First Department of Oncology, Zhumadian Central Hospital, No. 747 Zhonghua Road, Zhumadian 463000,

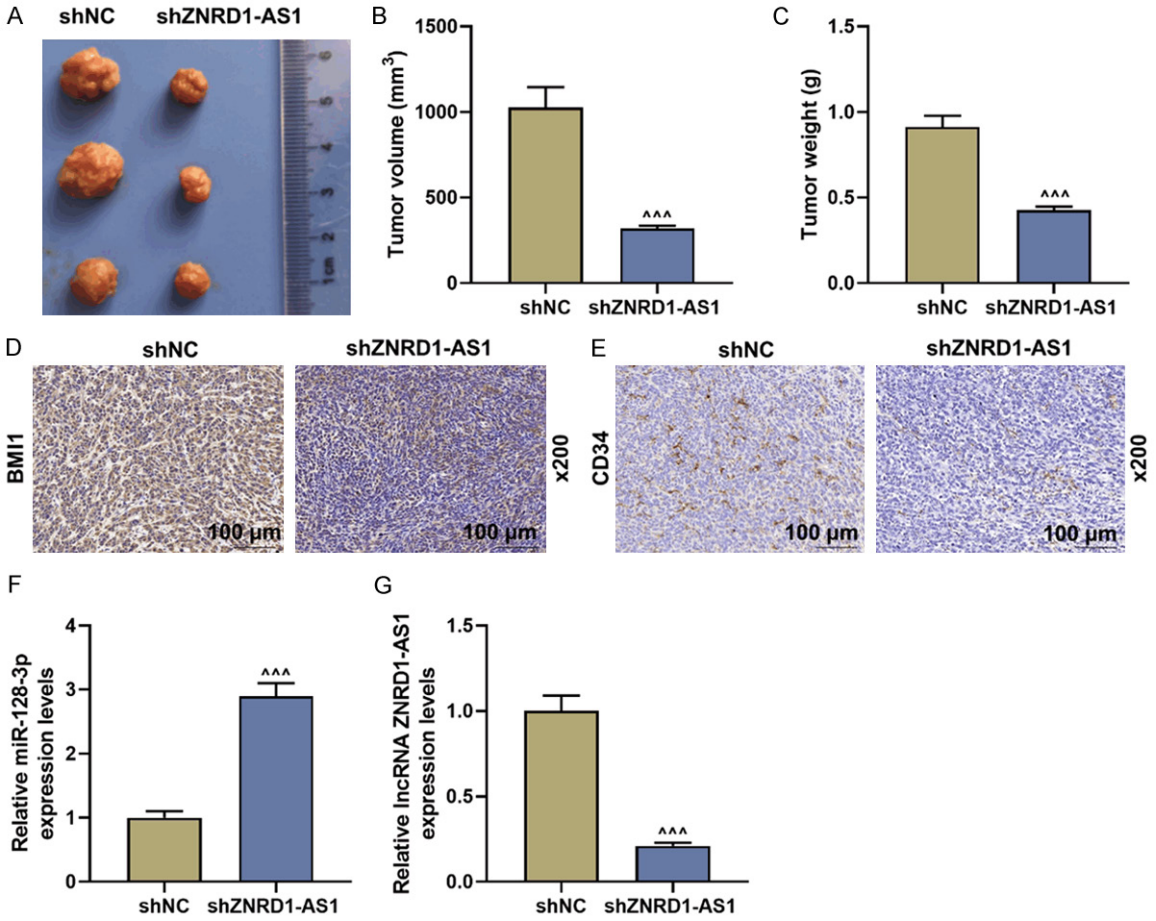

Figure 8. ShZNRD1-AS1 inhibited tumor growth via miR-128-3p/BMI1. A-C. The subcutaneous transplantation tumor experiment was used to detect the effect of ZNRD1-AS1 on tumor growth in the mice (n = 6/each group). D, E. Immunohistochemistry was used to detect BMI1 and vascular density marker CD34 in shNC and shZNRD1-AS1 groups. F, G. The expression of miR-128-3p and ZNRD1-AS1 in each group was evaluated by RT-qPCR. ^^^$P < 0.001$ vs. shNC.

Henan, China. Tel: +86-0396-2726207; E-mail: yangguanghua_ygh1@163.com

References

[1] Dimaras H, Corson TW, Cobrinik D, White A, Zhao J, Munier FL, Abramson DH, Shields CL, Chantada GL, Njuguna F and Gallie BL. Retinoblastoma. Nat Rev Dis Primers 2015; 1: 15021.

[2] Francis JH, Roosipu N, Levin AM, Brodie SE, Dunkel IJ, Gobin YP and Abramson DH. Current treatment of bilateral retinoblastoma: the impact of intraarterial and intravitreous chemotherapy. Neoplasia 2018; 20: 757-763.

[3] Fabian ID, Johnson KP, Stacey AW, Sagoo MS and Reddy MA. Focal laser treatment in addition to chemotherapy for retinoblastoma. Cochrane Database Syst Rev 2017; 6: CD012366.

[4] Abramson DH, Shields CL, Munier FL and Chantada GL. Treatment of retinoblastoma in 2015: agreement and disagreement. JAMA Ophthalmol 2015; 133: 1341-1347.

[5] Fabian ID, Onadim Z, Karaa E, Duncan C, Chowdhury T, Scheimberg I, Ohnuma SI, Reddy MA and Sagoo MS. The management of retinoblastoma. Oncogene 2018; 37: 1551-1560.

[6] Yan B, Yao J, Liu JY, Li XM, Wang XQ, Li YJ, Tao ZF, Song YC, Chen Q and Jiang Q. lncRNA-MIAT regulates microvascular dysfunction by functioning as a competing endogenous RNA. Circ Res 2015; 116: 1143-1156.

[7] Shan K, Jiang Q, Wang XQ, Wang YN, Yang H, Yao MD, Liu C, Li XM, Yao J, Liu B, Zhang YY, J Y and Yan B. Role of long non-coding RNA-RNCR3 in atherosclerosis-related vascular dysfunction. Cell Death Dis 2016; 7: e2248.

[8] Liu C, Li CP, Wang JJ, Shan K, Liu X and Yan B. RNCR3 knockdown inhibits diabetes mellitus-

induced retinal reactive gliosis. Biochem Biophys Res Commun 2016; 479: 198-203.
[9] Liu JY, Yao J, Li XM, Song YC, Wang XQ, Li YJ, Yan B and Jiang Q. Pathogenic role of lncRNA-MALAT1 in endothelial cell dysfunction in diabetes mellitus. Cell Death Dis 2014; 5: e1506.
[10] Yang M and Wei W. Long non-coding RNAs in retinoblastoma. Pathol Res Pract 2019; 215: 152435.
[11] Su S, Gao J, Wang T, Wang J, Li H and Wang Z. Long non-coding RNA BANCR regulates growth and metastasis and is associated with poor prognosis in retinoblastoma. Tumour Biol 2015; 36: 7205-7211.
[12] Dong C, Liu S, Lv Y, Zhang C, Gao H, Tan L and Wang H. Long non-coding RNA HOTAIR regulates proliferation and invasion via activating Notch signalling pathway in retinoblastoma. J Biosci 2016; 41: 677-687.
[13] Wen J, Liu Y, Liu J, Liu L, Song C, Han J, Zhu L, Wang C, Chen J, Zhai X, Shen H and Hu Z. Expression quantitative trait loci in long noncoding RNA ZNRD1-AS1 influence both HBV infection and hepatocellular carcinoma development. Mol Carcinog 2015; 54: 1275-1282.
[14] Peng JT and Li MC. A functional Cis-eQTL locus in lncRNA ZNRD1-AS1 contributes to the susceptibility of endometrial cancer. Eur Rev Med Pharmacol Sci 2019; 23: 7802-7807.
[15] Wang Q, Hu X, Du M, Lu Z, Yan K, Zhao D, Jiang N, Peng Y, He X and Yin L. ZNRD1-AS1 promotes nasopharyngeal carcinoma cell invasion and metastasis by regulating the miR-335-ROCK1 axis. Onco Targets Ther 2020; 13: 4779-4790.
[16] Gudiseva HV, Berry JL, Polski A, Tummina SJ and O'Brien JM. Next-generation technologies and strategies for the management of retinoblastoma. Genes (Basel) 2019; 10: 1032.
[17] Kettunen J, Tukiainen T, Sarin AP, Ortega-Alonso A, Tikkanen E, Lyytikainen LP, Kangas AJ, Soininen P, Wurtz P, Silander K, Dick DM, Rose RJ, Savolainen MJ, Viikari J, Kahonen M, Lehtimaki T, Pietilainen KH, Inouye M, McCarthy MI, Jula A, Eriksson J, Raitakari OT, Salomaa V, Kaprio J, Jarvelin MR, Peltonen L, Perola M, Freimer NB, Ala-Korpela M, Palotie A and Ripatti S. Genome-wide association study identifies multiple loci influencing human serum metabolite levels. Nat Genet 2012; 44: 269-276.
[18] Wang M, Yang C, Liu X, Zheng J, Xue Y, Ruan X, Shen S, Wang D, Li Z, Cai H and Liu Y. An upstream open reading frame regulates vasculogenic mimicry of glioma via ZNRD1-AS1/miR-499a-5p/ELF1/EMI1 pathway. J Cell Mol Med 2020; 24: 6120-6136.
[19] Kim HW, Jeong D, Ham J, Kim H, Ji HW, Choi EH and Kim SJ. ZNRD1 and its antisense long noncoding RNA ZNRD1-AS1 are oppositely regulated by cold atmospheric plasma in breast cancer cells. Oxid Med Cell Longev 2020; 2020: 9490567.
[20] Gao Z, Li S, Zhou X, Li H and He S. Knockdown of lncRNA ZNRD1-AS1 inhibits progression of bladder cancer by regulating miR-194 and ZEB1. Cancer Med 2020; 9: 7695-7705.
[21] Peng WX, Koirala P and Mo YY. LncRNA-mediated regulation of cell signaling in cancer. Oncogene 2017; 36: 5661-5667.
[22] Wang JX, Yang Y and Li K. Long noncoding RNA DANCR aggravates retinoblastoma through miR-34c and miR-613 by targeting MMP-9. J Cell Physiol 2018; 233: 6986-6995.
[23] Long Y, Wang X, Youmans DT and Cech TR. How do lncRNAs regulate transcription? Sci Adv 2017; 3: eaao2110.
[24] Liu T, Zhang X, Du L, Wang Y, Liu X, Tian H, Wang L, Li P, Zhao Y, Duan W, Xie Y, Sun Z and Wang C. Exosome-transmitted miR-128-3p increase chemosensitivity of oxaliplatin-resistant colorectal cancer. Mol Cancer 2019; 18: 43.
[25] Guo XL, Wang HB, Yong JK, Zhong J and Li QH. MiR-128-3p overexpression sensitizes hepatocellular carcinoma cells to sorafenib induced apoptosis through regulating DJ-1. Eur Rev Med Pharmacol Sci 2018; 22: 6667-6677.
[26] Pan J, Zhou C, Zhao X, He J, Tian H, Shen W, Han Y, Chen J, Fang S, Meng X, Jin X and Gong Z. A two-miRNA signature (miR-33a-5p and miR-128-3p) in whole blood as potential biomarker for early diagnosis of lung cancer. Sci Rep 2018; 8: 16699.
[27] Mou T, Luo Y, Huang Z, Zheng D, Pu X, Shen A, Pu J, Li T, Dai J, Chen W and Wu Z. Inhibition of microRNA-128-3p alleviates liver ischaemia-reperfusion injury in mice through repressing the Rnd3/NF-kappaB axis. Innate Immun 2020; 26: 528-536.
[28] Lu TX and Rothenberg ME. MicroRNA. J Allergy Clin Immunol 2018; 141: 1202-1207.
[29] Tu Y, Gao X, Li G, Fu H, Cui D, Liu H, Jin W and Zhang Y. MicroRNA-218 inhibits glioma invasion, migration, proliferation, and cancer stem-like cell self-renewal by targeting the polycomb group gene Bmi1. Cancer Res 2013; 73: 6046-6055.
[30] Flamier A, Abdouh M, Hamam R, Barabino A, Patel N, Gao A, Hanna R and Bernier G. Off-target effect of the BMI1 inhibitor PTC596 drives epithelial-mesenchymal transition in glioblastoma multiforme. NPJ Precis Oncol 2020; 4: 1.
[31] Ke B, Ye K and Cheng S. ALKBH2 inhibition alleviates malignancy in colorectal cancer by regulating BMI1-mediated activation of NF-κB pathway. World J Surg Oncol 2020; 18: 328.

[32] Yu J, Chen L, Bao Z, Liu Y, Liu G, Li F and Li L. BMI-1 promotes invasion and metastasis in endometrial adenocarcinoma and is a poor prognostic factor. Oncol Rep 2020; 43: 1630-1640.
[33] Hossain S, Iwasa H, Sarkar A, Maruyama J, Arimoto-Matsuzaki K and Hata Y. The RASSF6 tumor suppressor protein regulates apoptosis and cell cycle progression via retinoblastoma protein. Mol Cell Biol 2018; 38: e00046-18.
[34] Dimri M, Carroll JD, Cho JH and Dimri GP. microRNA-141 regulates BMI1 expression and induces senescence in human diploid fibroblasts. Cell Cycle 2013; 12: 3537-3546.
[35] Wu SQ, Xu ZZ, Niu WY, Huang HB and Zhan R. ShRNA-mediated Bmi-1 silencing sensitizes multiple myeloma cells to bortezomib. Int J Mol Med 2014; 34: 616-623.
[36] Ganaie AA, Beigh FH, Astone M, Ferrari MG, Maqbool R, Umbreen S, Parray AS, Siddique HR, Hussain T, Murugan P, Morrissey C, Koochekpour S, Deng Y, Konety BR, Hoeppner LH and Saleem M. BMI1 drives metastasis of prostate cancer in caucasian and African-American men and is a potential therapeutic target: hypothesis tested in race-specific models. Clin Cancer Res 2018; 24: 6421-6432.
[37] Wang YD, Su YJ, Li JY, Yao XC and Liang GJ. Rapamycin, a mTOR inhibitor, induced growth inhibition in retinoblastoma Y79 cell via down-regulation of Bmi-1. Int J Clin Exp Pathol 2015; 8: 5182-5188.
[38] Zhou J, Chen A, Wang Z, Zhang J, Chen H, Zhang H, Wang R, Miao D and Jin J. Bmi-1 determines the stemness of renal stem or progenitor cells. Biochem Biophys Res Commun 2020; 529: 1165-1172.
[39] Zhang Y and Weinberg RA. Epithelial-to-mesenchymal transition in cancer: complexity and opportunities. Front Med 2018; 12: 361-373.